DESIGN OF A REVERSIBLE HEAT PUMP/ORGANIC RANKINE CYCLE UNIT FOR A RENEWABLES-BASED TRIGENERATION SYSTEM

Antonios Charalampidis*, Konstantinos Braimakis, Sotirios Karellas

National Technical University of Athens, Laboratory of Steam Boilers and Thermal Plants, Athens, Greece

*Corresponding Author: antonishar@mail.ntua.gr

ABSTRACT

Reversible heat pump/organic Rankine cycle (RHP/ORC) systems have been lately brought to the forefront of two main applications. The first involves the provision of useful heating or cooling and the exploitation of external heat sources for power production, whereas the second deals with energy storage, where heat is primarily produced to be stored and then utilized for power generation to compensate the mismatch between generation and demand. In the present study, the design and the seasonal performance evaluation of a micro-scale, renewable energy-based trigeneration system having an RHP/ORC unit at its core are presented, where the two aforementioned concepts can be combined. The system operates either as a heat pump for low-temperature heating driven by solar heat and for cooling coupled with an adsorption chiller in a cascade configuration or as a stand-alone chiller, or as an ORC valorizing solar and/or biomass heat up to 120 °C. The design of the prototype system is hereby presented, including system modeling and working fluid selection, system architecture design and equipment sizing. Based on the simulations, the flexible design of the system allows for efficient performance under the main identified operating modes, reaching a seasonal energy efficiency ratio (SEER) and seasonal coefficient of performance (SCOP) of 3.63 and 4.25 for an average climate, as well as a maximum nominal ORC efficiency up to 5.90%.

1 INTRODUCTION

Reversible heat pump/organic Rankine cycle (ORC) systems (RHP/ORCs) have recently gained significant research interest, considering that the power generating ORC is essentially a heat pump operating in reverse, using mostly the same primary components (Dumont *et al.*, 2015), allowing for an integrated system.

On the one hand, RHP/ORCs have been proposed for combined heat and power (CHP) generation through the utilization of excess heat (e.g. solar or industrial waste heat). This concept was proposed by Schimpf and Span (2015) for a residential RHP/ORC system operating with R134a and driven by flat-plate solar collectors, including a vertical ground heat exchanger for the production of space heating, domestic hot water (DHW) and electricity. A techno-economic study revealed that the modification of the heat pump to also operate as an ORC could deliver up to 9% of the annual electricity demand, resulting in a payback period of around 20 years. A slightly different RHP/ORC architecture hosting a four-way valve was designed by Quoilin *et al.* (2016) and experimentally tested by Dumont *et al.* (2015) to meet the space heating and electricity demand of a building with solar collectors and a horizontal ground heat exchanger by harnessing the excess solar heat. Based on the results that were obtained with R134a as working fluid, the Coefficient of Performance (COP) and ORC efficiency reached 7.1 and 5.3%, respectively. Apart from the residential sector, studies have been conducted for other applications. Mateu-Royo *et al.* (2019) examined the application of a high-temperature system utilizing low-temperature waste heat. The authors performed a multi-objective optimization for the selection of an environmentally friendly working fluid and the compressor/expander built-in volume ratio under different scenarios in order to maximize the energy efficiency and the compactness of the system. It was concluded that the use of R1233zd(E) resulted in adequate performance and small volume footprint of the system. In another application, an RHP/ORC for combined air-conditioning and torque supply to

the shaft of a passage car tank by extracting heat from the engine cooling system has been investigated by Di Cairano *et al.* (2020). The assessment was based on experimentally validated dynamic simulations for different cities. It was found that a reduction in fuel consumption from 1 to 2% was possible, while the system was more appropriate in cold climates where cooling needs were lower, and thus the operating time of the ORC was extended.

On the other hand, RHP/ORCs have also been suggested for electricity storage in the form of heat (power-to-heat – Carnot Battery). Staub *et al.* (2018) investigated a system comprising a high-temperature heat pump for the production of hot water utilizing waste heat and excess renewable electricity, with the stored heat being used for driving an ORC for power production. The simulations indicated that a roundtrip efficiency of up to 70% could be attained. Dumont and Lemort (2020) introduced the Thermally Integrated Carnot Battery concept for RHP/ORCs. The authors developed performance maps of the system implying that roundtrip efficiencies above 100% could be achieved by exploiting waste or ambient heat to increase the high temperature or decrease the low temperature of the ORC, respectively. Moreover, the authors outlined that the first option was more efficient leading to higher storage density. Eppinger *et al.* (2021) presented the design of a Carnot Battery system, with a rated compressor electrical power of 14.7 kW, placing emphasis on the working fluid selection and lubrication challenges. The described system used R1233zd(E) as working fluid and included two compression/expansion machines, a piston compressor used in charging mode and a twin-screw expander in discharging mode, to deal with the different pressure ratios of the heat pump and the ORC.

In the present work, the implementation of an RHP/ORC for combined heating cooling and power (CCHP) production and electricity storage into an innovative, integrated concept is investigated. The proposed system incorporates a thermally-driven chiller and is capable of utilizing multiple heat sources through the integration of various technologies, while it is currently being developed for field testing in two different locations. In the study, the design aspects of the system are highlighted, while its key performance specifications are discussed.

2 METHODOLOGY

2.1 Global system description

The designed RHP/ORC system is part of the global system described by Palomba *et al.* (2020), which aims at meeting the space heating (low-temperature underfloor heating at 35 °C), space cooling (low-temperature cooling at 7 °C), DHW and part of the electricity demand of a building in a flexible way by exclusively exploiting renewable energy. The global system is under development and will be tested in two pilot buildings, in Athens, Greece and Nuremberg, Germany.

The two prototypes are similar, with the Athens prototype being slightly more complex since it is additionally capable of solar cooling production, and consists of the following components. 25 m^2 evacuated tube solar collectors integrated with thermoelectric generators (TEGs) for harvesting solar energy (up to 90 °C) and generating low-power through the temperature difference applied to the TEGs terminals; A 15 kW pellet biomass boiler of two separate circuits providing 7 kW at 60-80 °C for space heating and DHW and 8 kW to the ORC at 100-120 °C for power generation; An RHP/ORC which operates in two modes: i) heat pump mode for the provision of 5 kW space heating (solar-assisted) and 4 kW of space cooling by rejecting heat at either the ambient or the evaporator of an adsorption chiller and ii) ORC mode for up to 1 kW power generation utilizing stored solar heat (above 80 °C) and/or high-temperature biomass heat (100-120 °C); A 5 kW adsorption chiller utilizing medium to high temperature solar heat (65-90 °C) to provide low-pressure water vapor to the directly coupled condenser of the RHP/ORC in heat pump mode to reduce its condensation temperature; Two sensible water tanks for thermal energy storage. One tank (short-term storage) stores solar heat which is supplied to the various circuits (space heating, DHW, RHP/ORC), while the other tank (buffer) is used for hot or cold storage depending on the season; A dry-cooler primarily used for rejecting heat from the condensers of the heat pump and the adsorption chiller and, secondarily, as heat source from the ambient for air-driven heating.

It is evident that the present system constitutes a sophisticated solution incorporating multiple technologies. Due to its complexity, several technical considerations arise. For instance, a detailed

control strategy is needed to optimize system performance. In addition, the relatively low technological maturity of some subsystems and their integration increases the risk of malfunctions. On the other hand, the large number of interchangeable subsystems minimizes the probability of the whole system being out of operation. These aspects are taken into account by the control platform by scheduling proactive maintenance measures, which will be analyzed in future studies, as the current work focuses on the design of the RHP/ORC.

2.2 Operating modes

The main operating modes of the global system are summarized below, depending on the output:

- **Space heating:** Space heating is primarily supplied by stored solar energy. If the stored solar energy is insufficient, heating is produced by the RHP/ORC, which operates as heat pump in solar-assisted (when limited stored solar energy is available) or stand-alone/air-driven (i.e. utilizing ambient heat) mode. In case of no stored solar heat and very low ambient temperatures, space heating is produced by the biomass boiler.
- **Space cooling:** When solar heat at a sufficient temperature (above 65 °C) is available, the space cooling is produced by the adsorption chiller in conjunction with the RHP/ORC, which operates as a heat pump. The two subsystems are connected in a cascade configuration (cascade chiller mode). More specifically, space cooling is produced by the RHP/ORC, while the solar-driven adsorption chiller is used for reducing the heat rejection temperature of the RHP/ORC, thus improving its performance. If the solar heat is insufficient, cooling is produced by the RHP/ORC which operates as a stand-alone heat pump, rejecting heat at the ambient (vapor compression).
- **DHW:** Domestic hot water is provided through the heat stored in the short-term storage tank, which is primarily derived from the solar collectors and secondarily, from the biomass boiler, which serves as an auxiliary on-demand energy source.
- **Electricity:** Electricity is mainly supplied by the grid. Nonetheless, if space heating/cooling needs are met and either the short-term storage tank (solar-driven mode) is charged or the biomass boiler is operational (biomass-driven/hybrid mode), heat is supplied to the RHP/ORC which operates in ORC mode. Otherwise, the thermoelectric generators are deployed.

The main operating modes for the RHP/ORC and the boundary conditions in terms of heat source, heat sink temperatures and heating/cooling capacities (condenser capacity for heating modes and evaporator capacity for cooling and ORC modes) are shown in Table 1. A lower heat sink temperature is defined in biomass-driven ORC modes because the boiler supplies the ORC only when it is operational, i.e. in winter or intermediate seasons, implying a lower ambient temperature.

Table 1: Boundary conditions of RHP/ORC operating modes

Operating mode	Heat source temperature In/Out (°C)	Heat sink temperature In/Out (°C)	Thermal capacity (kW)
Cascade chiller (#1)	12/7	20[*1]/–[*2]	4
Vapor compression (#2)	12/7	30/–[*2]	4
Solar-assisted heating (#3)	15/–[*2]	30/35	5
Air-driven heating (#4)	5/–[*2]	30/35	5
Solar-driven ORC (#5)	90/–[*2]	30/–[*2]	15
Biomass-driven ORC (#6)	90/–[*2]	15/–[*2]	15
Hybrid ORC (#7)	90/–[*2] & 110/–[*2]	15/–[*2]	15 (7 + 8)

[*1] in form of low-pressure water vapor

[*2] calculated internally

2.3 RHP/ORC configuration

The layout of the RHP/ORC system is depicted in Figure 1. In the figure, the solar-assisted heating and hybrid ORC operating modes are illustrated, along with the active branches, the flow direction, and the heat/power flow. It is apparent that the flow direction is reversed in heat pump and ORC modes, whereas the heat exchangers function interchangeably as evaporators or condensers and are distinguished by their pressure level in the system; low-pressure (LP) heat exchangers operate as evaporators in the heat

pump and as condensers in the ORC and high-pressure (HP) heat exchangers operate in reverse. The main components of the RHPC/ORC are the following:

- Three high-pressure plate heat exchangers; one for operating as heat pump condenser and solar-driven ORC evaporator (solar HEX), one for the biomass boiler (biomass HEX) and one as adsorption chiller evaporator/heat pump condenser (Sorption HEX).
- Two low-pressure plate heat exchangers; one as heat pump evaporator and ORC condenser and one exclusively as subcooler of the ORC to avoid pump cavitation.
- Two serially connected variable speed, open-drive scroll compressors/expanders of different swept volumes; one working exclusively in ORC (high-pressure) and another in both ORC and heat pump modes (low-pressure).
- An external liquid receiver with two branches activated by solenoid valves; one for moving refrigerant out of the system (pumpdown) and one for filling the system with refrigerant, in order to actively manage the refrigerant charge and prevent lubricating oil from accumulating in the receiver.
- Bypass branches with normally open solenoid valves for start-up and emergency stops.

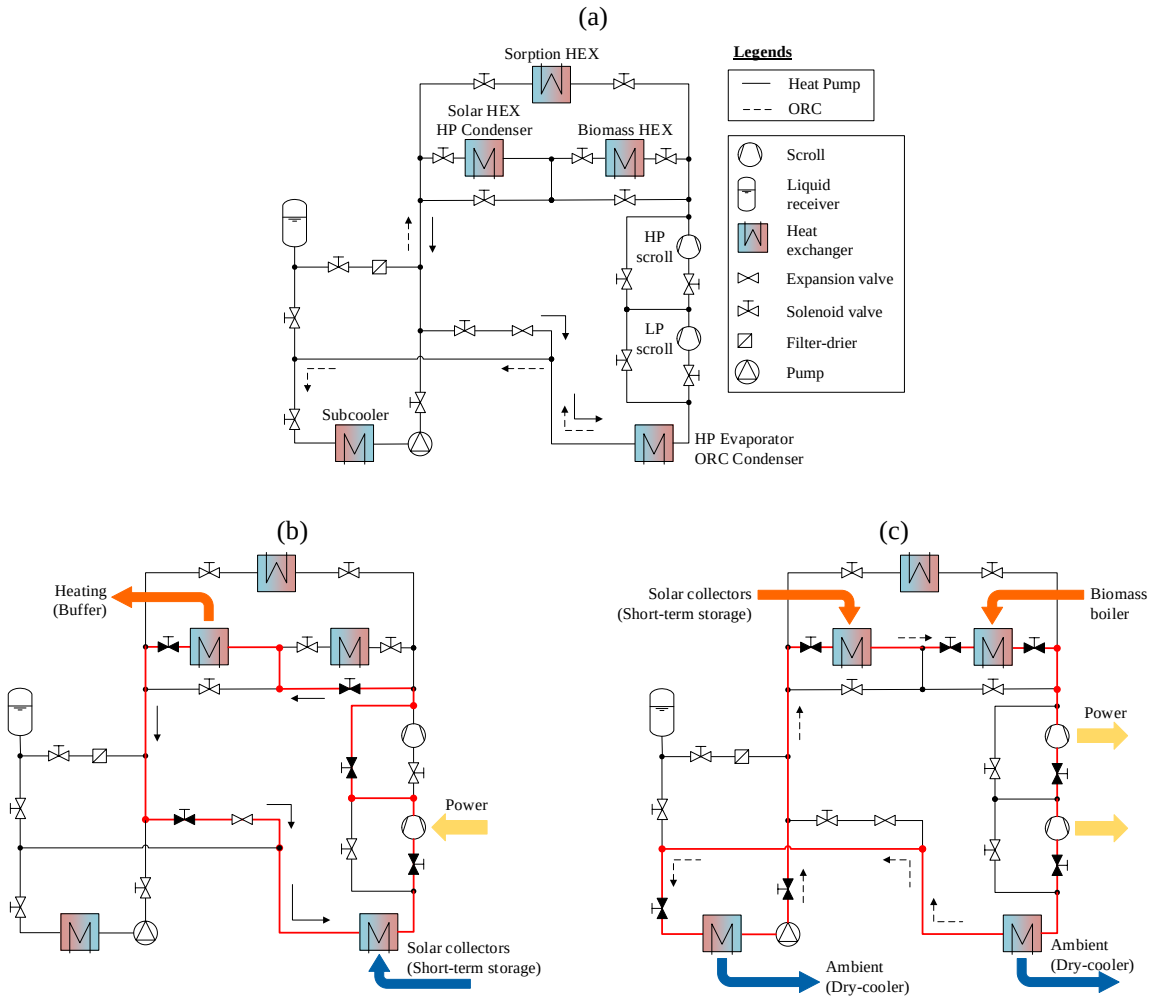

Figure 1: Layout of the RHP/ORC system (a), system operation in Mode 2 (b) and Mode 7 (c)

2.4 Working fluid

The use of refrigerants with zero Ozone Depletion Potential (ODP) and Global Warming Potential (GWP) below 10 was considered for the system. Given the fact that only subcritical cycles were concerned, fluids with critical temperatures above 100 °C were considered, since for these, biomass-driven ORC cycles are feasible without substantial superheating. Besides, flammability issues were taken into account. Finally, refrigerants for which the evaporation and condensation pressures in heat pump mode were too close (with a difference below 1 bar) were excluded to ensure the stable and proper

operation of the expansion valve. Finally, refrigerants with sub-atmospheric saturation pressures in the operating conditions were also not considered to prevent ambient air intake.

The performance of fluids meeting the above criteria was then calculated, i.e. the Coefficient of Performance (COP)/Energy Efficiency Ratio (EER) for heating and cooling respectively and net thermal efficiency of the ORC. The results of the screening process were obtained assuming constant superheating and subcooling (10 and 5 K for ORC and 5 K each for heat pump), pinch point values of 5 K in all heat exchangers and compressor/expander and pump efficiency, equal to 60 and 45%, respectively. R1234ze(E) was finally selected with a 6.25 EER and 5.42% efficiency for the biomass ORC. Its main properties (critical pressure and temperature, normal boiling point, saturation pressure at 20 °C, GWP, ODP and ASHRAE safety classification) are shown in Table 2.

Table 2: Basic properties of R1234ze(E) (Bell *et al.*, 2014)

p_{cr} (bar_a)	T_{cr} (°C)	NBP (°C)	$p_{sat,20\ °C}$ (bar_a)	GWP	ODP	ASHRAE safety class
36.36	109.37	-18.97	4.27	6	0	A2L

2.5 Modeling

Steady-state component models were developed and then connected for the selection and sizing of equipment components of the RHP/ORC, and the assessment of its seasonal performance.

- **Heat exchangers:** A moving boundary modeling methodology was followed, by separating the heat exchanger into regions depending on the state of the working fluid, i.e. single- or two-phase. Subsequently, the aforementioned heat exchanger regions were further divided into smaller zones. Two zones were used for single-phase regions and ten for two-phase. The Logarithmic Mean Temperature Difference method was applied in each zone *i* to obtain the heat exchanged within it, according to the zone overall heat transfer coefficient U_i:

$$U_i = \left(\frac{1}{a_{h,i}} + \frac{1}{a_{c,i}} + \frac{t_p}{k_p} + R_{f,tot} \right)^{-1} \quad (1)$$

with a_h, a_c being the convective heat transfer coefficient of the hot and the cold fluid, respectively, t_p the thickness of the plate, k_p its thermal conductivity taken equal to 16.3 W/mK for AISI 316L stainless steel and $R_{f,tot}$ a fouling thermal resistance, assumed equal to $0.33 \cdot 10^{-4}$ m^2K/W according to manufacturer recommendation. The convective heat transfer coefficients were obtained for single-phase, evaporating and condensing flows from relevant studies (Thonon *et al.*, 1995; Longo *et al.*, 2015; Zhang *et al.*, 2019). Ultimately, the total pressure drop of each stream was calculated, induced by the ports/manifold and the plates, using single- and two-phase evaporation and condensation correlations from the literature (Martin, 1996; Yan and Lin, 1999; Tao and Ferreira, 2019).

- **Compressor:** The semi-empirical model of Lemort (2008) was used for simulating the compressor. According to the model, the compression is broken down into six simple thermodynamic processes, including heat exchange with the ambient, mixing with an internal leakage flow, a two-stage adiabatic compression and an outlet pressure drop. Besides the model's mechanical losses, expressed in terms of torque, a motor's efficiency and a power transmission efficiency were also included. The former was calculated via a polynomial correlation versus the part-load ratio of the power output, based on motors datasheets, while the latter was assumed constant, equal to 0.90. The model parameters were taken as in the original model (Lemort, 2008), except for the built-in volume ratio and the swept volume which were varied according to the specifications of the considered scroll machines.

- **Expander:** In a similar manner, the expander was modeled according to Lemort's model (Lemort *et al.*, 2009), which again takes into account performance degradation owing to pressure drops, heat and volumetric losses, under- and over- expansion, and mechanical losses. As stated above, additional motor and mechanical losses were incorporated and the parameters proposed by the model were adapted excluding the built-in volume ratio and the swept volume. The compressor and expander model parameters used in the study are summarized in Table 3.

Table 3: Parameters of compressor and expander semi-empirical models

Parameter	Compressor	Expander
Ambient heat transfer coefficient (W/K)	3.0	6.4
Supply heat transfer coefficient (W/K)	30.0	21.2
Exhaust heat transfer coefficient (W/K)	20.0	34.2
Leakage area (mm^2)	0.39	4.6
Inlet/Outlet port section (mm^2)	21.24	27.43
Nominal mass flow rate (kg/s)	0.091	0.120
Mechanical loss torque (Nm)	0.27	0.47
Motor nominal efficiency (–)	0.85	0.85
Power transmission efficiency (–)	0.90	0.90

- **Pump:** The volumetric pump of the system is modeled using performance maps of commercial models, in which the displaced volume flow rate $\dot{V}_{p,dis}$ and mechanical power input to the pump $\dot{W}_{p,m}$ are given in relation to the rotational speed and the pump pressure difference. The performance map of the finally selected diaphragm volumetric pump is depicted in Figure 2, where solid lines correspond to the displaced flow rate and dashed lines to the mechanical power.

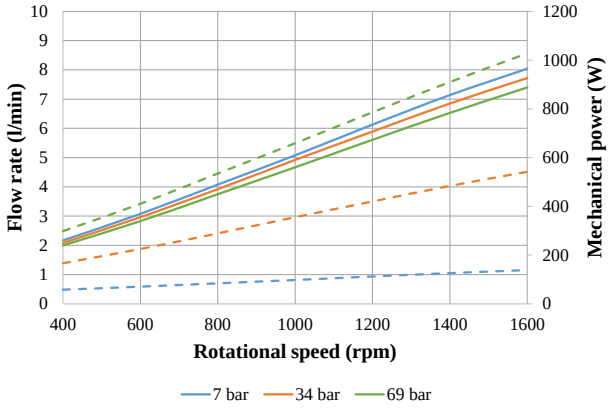

Figure 2: Performance map of the finally selected pump (flow rate in solid line, mechanical power in dashed line)

The total ($\eta_{p,tot}$) and volumetric ($\eta_{p,vol}$) efficiency of the pump are then calculated with respect to its rotational speed (N_p) and swept volume ($V_{s,p}$), and the theoretical pressure difference between inlet and outlet (Δp_{th}), neglecting internal pressure drops and other irreversibilities:

$$\eta_{p,tot} = \frac{N_p V_{s,p} \Delta p_{th}}{\dot{W}_{p,m}} \tag{2}$$

$$\eta_{p,vol} = \frac{N_p V_{s,p}}{\dot{V}_{p,dis}} \tag{3}$$

Using equations (2) and (3), correlations of the total and volumetric efficiencies as a function of the rotational speed and pressure difference were derived. Assuming an adiabatic process, the mechanical power provided to the fluid is equal to the increase of fluid's specific enthalpy (Equation 4), assuming a mechanical efficiency of the pump ($\eta_{p,m}$) of 0.90.

$$\dot{m}\Delta h_p = \dot{W}_{p,m}\eta_{p,m} \tag{4}$$

- **Expansion valve:** The expansion valve is simply modeled by means of its flow coefficient K_V which is either given by manufacturers or can be extracted by their datasheets.

3 RESULTS AND DISCUSSION

3.1 Sizing and components selection

The sizing of the system was conducted taking into account the nominal conditions reported in Table 1. As shown by Palomba *et al.* (2020), all operating modes of the RHP/ORC are of major importance

and therefore were equally considered in sizing. Superheating, subcooling and pinch point values equal to 5 K were defined for the heat pump and 5, 3 and 5 K for the ORC, respectively. Regarding the superheating, it is needed to ensure single-phase vapor supply at the inlet of the compressor/expander and prevent liquid formation, whereas the role of subcooling is twofold. In heat pump mode, it ensures liquid supply at the inlet of the expansion valve enhancing its stability, while in ORC mode it is required to mitigate the risk of cavitation, as previously mentioned. Notably, in heat pump cooling mode subcooling increases the cooling capacity whereas in ORC mode, it reduces the ORC efficiency. The selection and design aspects of the key components are discussed below:

- **Heat exchangers:** Brazed plate heat exchangers were selected. In addition to the heat transfer requirement under all operating modes, a maximum allowable pressure drop was set to 200 mbar for water, and 200 or 1000 mbar (in case a distributor is used) for the refrigerant. Regarding the subcooler, in order to avoid cavitation at the pump inlet, a maximum pressure drop of 50 mbar was considered. Finally, it is noted that general-purpose heat exchangers were selected in all cases, to ensure their consistent and stable performance (as far as heat transfer and pressure drop is concerned), during their alternating operation as evaporators and condensers.
- **Compressor/Expander:** Open-drive, variable speed, off-the-shelf automotive scroll compressors were selected since they can be easily modified to operate also as expanders in ORC mode, by removing their discharge check valve during their installation and by changing the flow direction and their direction of rotation during operation. Scrolls with built-in volume ratios better matching the operating volume ratios were chosen. Finally, smaller swept volumes were preferred to ensure operation at higher speeds thus increasing their volumetric efficiency.
- **Pump:** Volumetric pumps of different manufacturers were evaluated. Among various types, diaphragm pumps were finally selected owing to their higher cavitation resistance ($NPSH_r$ < 3 m) at the specified flow range (below 5 l/min) and their hermetic design which eliminates the risk of leakages of the slightly flammable R1234ze(E).
- **Expansion valve:** An electronic expansion valve with a bipolar stepper motor was selected, which is suitable for the selected refrigerant and features a wide capacity range, ensuring stable superheating control.

The equipment specifications of the final sizing and the main performance indicators under all modes (COP for heating, EER for cooling and total efficiency for the ORC, expressed as the ratio of net electrical power divided by the heat input in the evaporator) are shown in Table 4 and Table 5. The modes numbering shown in Table 5 is the same with that presented in Table 1. For clarity's sake, power consumption in modes 1-4 is indicated with a minus sign to differentiate from power generation occurring in modes 5-7. Apparently, the system attains adequate performance under all operating modes, with a COP of 4.58 (solar-assisted heating), an EER of 5.10 (cascade chiller), and an efficiency of 5.90% (hybrid ORC). Concluding, efficient operation at both low and high pressure ratios is achieved, maintaining medium to high rotational speeds of the scrolls (above 1500 rpm) under all operating conditions, minimizing volumetric losses.

Table 4: Equipment specifications of the reversible HP/ORC

Specification	**Value**
High-pressure scroll swept volume (cm^3)	18.0
High-pressure scroll built-in volume ratio (–)	2.2
Low-pressure scroll swept volume (cm^3)	60.0
Low-pressure scroll built-in volume ratio (–)	2.4
Pump swept volume (cm^3)	5.5
Pump $NPSH_r$ at 1000 rpm (m)	2.3
Expansion valve K_v range (m^3/h)	0.012-0.12
High-pressure HEXs surface area (m^2)	1.02
Low-pressure HEX surface area (m^2)	2.04
Subcooler surface area (m^2)	0.58

Table 5: Key performance indicators in all design points under nominal conditions

Property	**#1**	**#2**	**#3**	**#4**	**#5**	**#6**	**#7**
Mass flow rate (g/s)	25.6	28.1	28.8	27.5	81.1	72.9	72.0
Evaporation pressure (bar_a)	2.33	2.33	2.59	1.79	20.07	24.75	30.26
Condensation pressure (bar_a)	5.78	7.66	7.66	7.66	7.26	4.69	4.69
Intermediate pressure (bar_a)	–	–	–	–	–	11.47	12.10
Pump total efficiency (%)	–	–	–	–	38.72	41.13	49.23
HP scroll total efficiency (%)	–	–	–	–	51.65	30.71	51.66
LP scroll total efficiency (%)	57.06	56.06	57.46	51.93	–	51.66	52.18
COP/EER/Net efficiency (–/%)	5.10	3.48	4.58	3.25	3.80	4.45	5.90
Power consumption/generation (W)	-784.9	-1150.2	-1047.6	-1475.7	570.4	668.1	884.6

3.2 Seasonal performance

As previously stated, the investigated prototype system will be tested in two pilot buildings currently being built in Greece and Germany. The heating and cooling consumption profiles in these locations are significantly different. Meanwhile only the pilot system to be tested in Greece will feature an adsorption chiller. Besides, the exact operating time of each mode in the two sites is not defined yet in the absence of a detailed control strategy. Furthermore, considering that the heat input to the ORC is expected to remain roughly constant thanks to the short-term storage tank and the supplementary heat from the biomass boiler, the main seasonal fluctuation of the system is due to the different operating modes of the heat pump. The seasonal evaluation in the present work was therefore focused on two main modes, namely solar-assisted heating and stand-alone cooling, excluding the cascade mode, which only concerns the Greek pilot system and presupposes the definition of a detailed control strategy.

An approach similar to the Ecodesign (European Parliament, 2009) was applied for an average climate, representative to the German case. Despite the use of storage tanks, the part load behavior of the system under variable ambient and supply temperatures was taken into account, as it is common for the standardized characterization of heat pumps and chillers.

Specifically, the European legislative framework (European Parliament, 2016) for small-scale comfort chillers and heat pumps was used as a basis for calculating the Seasonal Energy Efficiency Ratio (SEER) for cooling and Seasonal Coefficient of Performance (SCOP) for heating, using average annual load profiles (Figure 3) with four reference points (A-D) of different conditions. Fixed water target temperatures equal to 35 °C for heating and 7 °C for cooling were imposed, along with variable water flow for maintaining a constant temperature difference of 5 K in each heat exchanger. The only difference to the Ecodesign is the evaporator water inlet temperature in heating, which is set to 15 °C instead of 10 °C, representing solar-assisted operation. The simulated conditions are shown in Table 6.

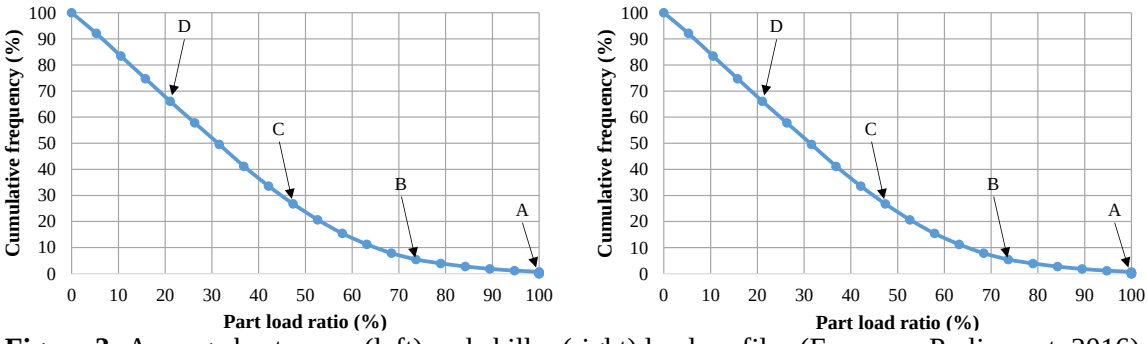

Figure 3: Average heat pump (left) and chiller (right) load profiles (European Parliament, 2016)

Table 6: Reference point conditions for seasonal performance evaluation

Property	**Solar-assisted heating**				**Stand-alone cooling**			
	A	**B**	**C**	**D**	**A**	**B**	**C**	**D**
Part load ratio (%)	88	54	35	15	100	74	47	21
Cumulative frequency (%)	1.0	24.6	58.5	89.8	0.7	5.4	26.7	66.1
Condenser In/Out (°C)	30/35	30/35	30/35	30/35	30/35	26/31	22/27	18/23
Evaporator In/Out (°C)	15/10	15/10	15/10	15/10	12/7	12/7	12/7	12/7

The simulation results indicate the sufficient seasonal performance in both operating modes of the heat pump. On the one hand, an SCOP of 4.25 was attained, which is higher than the minimum requirement of 3.33 (European Parliament, 2016). With regard to cooling operation, an SEER of 3.63 was reported, which is lower than the minimum standard of 5.20 (European Parliament, 2016). This is because of the very low mechanical power needed beyond point D, which reduces the efficiency of the induction motor owing to its very low part load ratio (below 10%). More specifically, the EER ranges from 5.17 to 2.54 between points A and D, with motor efficiency being reduced from 84.5 % to 28.7%, respectively. However, the operation in conjunction with thermal storage is anticipated to greatly reduce the highly part-load operation regime of the heat pump, improving its seasonal performance by avoiding the aforementioned part-load losses of the compressor motor. Furthermore, improved performance is expected after the adaption of the cascade chiller in southern climates thanks to the reduced temperature lift of the heat pump. In general, the low efficiency of the compressor motor under low loads is partly compensated by the high compressor efficiency (excluding motor) which ranges from 57.6 to 53.1%. Additionally, the large heat transfer area of the heat exchangers which resulted from the ORC sizing, due to its higher capacities, enhances heat transfer in heat pump modes. In this manner, the condensation and evaporation temperatures approach to water temperatures, thus reducing the operating pressure ratio is and enhancing the efficiency. Although these calculations are preliminary and need to be validated, it is envisaged that the seasonal performance of the reversible system is acceptable, even under much diverse operating conditions.

The results of the present work are compared with those of the studies by Schimpf and Span (2015) and Quoilin *et al.* (2016), which are oriented towards similar, micro-scale residential applications. With regard to the former, an RHP/ORC system providing 3.78 to 6.49 kW of solar-assisted heating and DHW at 40-60 °C in heat pump mode and 0.17 to 0.23 kW in ORC mode when driven by 12 m^2 of solar collectors at 60-90 °C was assessed. Simulations revealed an SCOP of 3.68-3.92 and an average ORC thermal efficiency of 5.8-6.0%, for different locations. Concerning the latter, an RHP/ORC was studied, utilizing solar heat for the production of up to 17.3 kW of space heating at 60 °C in heat pump mode and 4.73 kW (nominal) in ORC mode at an evaporation temperature of 90 °C. A nominal COP of 4.2 and an ORC efficiency of 7.6% were reported, while an SCOP of 2.70 was calculated. Compared to results of these studies, a higher SCOP is hereby expected whereas the nominal ORC efficiency is acceptable, especially considering that the selected refrigerant was not optimally selected for this mode due to technical limitations set by heat pump operation.

4 CONCLUSIONS

This study presented the design of a reversible heat pump/ORC system integrated into a hybrid trigeneration system driven by biomass and solar energy. Firstly, the main operating modes of the system along with their boundary conditions were defined. Based on the system specifications and boundary conditions, R1234ze(E) was selected as the working fluid as it represented the best trade-off between performance, safety and stable and controllable operation. In addition, a flexible architecture was adapted hosting multiple heat exchangers, two modified scroll compressors and a liquid receiver. The system operation was simulated and its key components were sized while its nominal and seasonal performance were calculated. The thermal efficiency of the system in ORC mode was 5.90%, while the COP and EER of the system in heat pump mode were above 4.50. The seasonal performance evaluation revealed that efficient operation is expected, as the flexible design of the system compensates for the inefficiencies occurring due to extensive part-load operation.

Ultimately, the thermally integrated Carnot Battery concept of storing cold water in the buffer tank when electricity prices are low (e.g. night) in order to enhance the thermal efficiency of the system in ORC mode was not investigated, however, it constitutes one of the main capabilities of the global system and a main future work recommendation.

REFERENCES

Bell, I.H., Wronski, J., Quoilin, S., Lemort, V., 2014, Pure and pseudo-pure fluid thermophysical property evaluation and the open-source thermophysical property library CoolProp, *Industrial & engineering chemistry research*, vol. 53, no. 6, p. 2498-2508.

Di Cairano, L., Nader, W.B., Nemer, M., 2020, Assessing fuel consumption reduction in Revercycle, a reversible mobile air conditioning/Organic Rankine Cycle system, *Energy*, vol. 210, p. 118588.

Dumont, O., Lemort, V., 2020, Mapping of performance of pumped thermal energy storage (Carnot battery) using waste heat recovery, *Energy*, vol. 211, p. 118963.

Dumont, O., Quoilin, S., Lemort, V., 2015, Experimental investigation of a reversible heat pump/organic Rankine cycle unit designed to be coupled with a passive house to get a Net Zero Energy Building, *International journal of refrigeration*, vol. 54, p. 190-203.

Eppinger, B., Steger, D., Regensburger, C., Karl, J., Schlücker, E., Will, S., 2021, Carnot battery: Simulation and design of a reversible heat pump-organic Rankine cycle pilot plant, *Appl. Energy*, vol. 288, p. 116650.

European Parliament, Council of the European Union. Directive 2009/125/EC of the European Parliament and of the Council of 21 October 2009. 2009.

European Parliament, Council of the European Union. Commission Regulation (EU) 2016/2281 of 30 November 2016. 2016.

Lemort, V., 2008, Contribution to the characterization of scroll machines in compressor and expander modes, *Liege: University of Liege-Belgium*, p.

Lemort, V., Quoilin, S., Cuevas, C., Lebrun, J., 2009, Testing and modeling a scroll expander integrated into an Organic Rankine Cycle, *Appl. Therm. Eng.*, vol. 29, no. 14-15, p. 3094-3102.

Longo, G.A., Mancin, S., Righetti, G., Zilio, C., 2015, A new model for refrigerant boiling inside Brazed Plate Heat Exchangers (BPHEs), *International Journal of Heat and Mass Transfer*, vol. 91, p. 144-149.

Martin, H., 1996, A theoretical approach to predict the performance of chevron-type plate heat exchangers, *Chemical Engineering and Processing: Process Intensification*, vol. 35, no. 4, p. 301-310.

Mateu-Royo, C., Mota-Babiloni, A., Navarro-Esbrí, J., Peris, B., Moles, F., Amat-Albuixech, M., 2019, Multi-objective optimization of a novel reversible High-Temperature Heat Pump-Organic Rankine Cycle (HTHP-ORC) for industrial low-grade waste heat recovery, *Energy Convers. Manage.*, vol. 197, p. 111908.

Palomba, V., Borri, E., Charalampidis, A., Frazzica, A., Cabeza, L.F., Karellas, S., 2020, Implementation of a solar-biomass system for multi-family houses: Towards 100% renewable energy utilization, *Renew. Energ.*, vol. 166, p. 190-209.

Quoilin, S., Dumont, O., Harley Hansen, K., Lemort, V., 2016, Design, modeling, and performance optimization of a reversible heat pump/organic Rankine cycle system for domestic application, *Journal of Engineering for Gas Turbines and Power*, vol. 138, no. 1, p.

Schimpf, S., Span, R., 2015, Simulation of a solar assisted combined heat pump–Organic rankine cycle system, *Energy Convers. Manage.*, vol. 102, p. 151-160.

Staub, S., Bazan, P., Braimakis, K., Müller, D., Regensburger, C., Scharrer, D., Schmitt, B., Steger, D., German, R., Karellas, S., 2018, Reversible heat pump–organic Rankine cycle systems for the storage of renewable electricity, *Energies*, vol. 11, no. 6, p. 1352.

Tao, X., Ferreira, C.A.I., 2019, Heat transfer and frictional pressure drop during condensation in plate heat exchangers: Assessment of correlations and a new method, *International Journal of Heat and Mass Transfer*, vol. 135, p. 996-1012.

Thonon, B., Vidil, R., Marvillet, C., 1995, Recent research and developments in plate heat exchangers, *Journal of Enhanced heat transfer*, vol. 2, no. 1-2, p.

Yan, Y.-Y., Lin, T.-F., 1999, Evaporation Heat Transfer and Pressure Drop of Refrigerant R-134a in a Plate Heat Exchanger, *Journal of Heat Transfer*, vol. 121, no. 1, p. 118-127.

Zhang, J., Kærn, M.R., Ommen, T., Elmegaard, B., Haglind, F., 2019, Condensation heat transfer and pressure drop characteristics of R134a, R1234ze (E), R245fa and R1233zd (E) in a plate heat exchanger, *International Journal of Heat and Mass Transfer*, vol. 128, p. 136-149.

ACKNOWLEDGEMENT

This study has been performed within the framework of the SolBio-Rev project, funded by the European Union's Horizon 2020 research and innovation program, under grant agreement No. 814945.